Surface states and photoemission of magnetic multilayer systems

S. V. Halilov, J. Henk, T. Scheunemann, and R. Feder
Theoretische Festkörperphysik, Universität Duisburg, 47048 Duisburg, Germany
(Received 15 December 1994; revised manuscript received 26 May 1995)

Key features of the surface electronic structure of magnetic multilayer systems are derived by analytical tight-binding Green function calculations for the simple model of a semi-infinite chain. In the case of antiferromagnetic (AFM) coupling, for which the bulk is macroscopically nonmagnetic, spin-up and spin-down surface states emerge in a bulk energy gap associated with the reduction of the Brillouin zone with respect to the nonmagnetic case. Explicit expressions for the surface state (ss) characteristics are obtained in terms of the main band parameters, displaying a strong sensitivity of the ss energies to deviations of the surface magnetic moments from the bulk ones. The simple model findings are confirmed and put on a quantitative footing by means of relativistic layer–Korringa-Kohn-Rostoker (KKR) calculations for multilayer systems $FePt_n(001)$ consisting of ferromagnetically ordered Fe monolayers coupled ferromagnetically (FM) or antiferromagnetically through $n = 0, 1, 2$ Pt layers. In particular, we retrieve for AFM coupling magnetic surface states in symmetry specific bulk energy gaps. For magnetization normal to the surface, normal valence-band photoemission spectra have been calculated by a relativistic one-step-model layer-KKR approach. Spin-polarized features in these spectra reflect the magnetic surface states. Due to spin-orbit coupling, they further exhibit an intensity asymmetry upon magnetization reversal known as magnetic circular dichroism (MCD). For AFM coupling, the surface-induced MCD can in fact be stronger than the MCD found for the corresponding FM system.

I. INTRODUCTION

Current interest in the electronic properties of magnetic films and multilayer systems (MS) involves details of the surface electronic structure and its manifestation in photoemission spectra, the various aspects of surface chemistry, surface transport phenomena, magneto-optics, and, in particular, perpendicular recording systems (cf., for example, Refs. 1–10 and references therein). A most widely studied class of MS is characterized by ferromagnetically ordered surface-parallel sets of monolayers with perpendicular magnetization, which are coupled either ferromagnetically or antiferromagnetically across nonmagnetic spacer layers (see Refs. 11–16 and references therein).

Particular insight can be gained by comparing the electronic structure of these ferromagnetic- and antiferromagnetic-type MS as arising by the exchange interaction from the paramagnetic (PM) phase. In the FM case, the magnetic exchange coupling leads to the usual spin splitting of the paramagnetic states, whereas in the antiferromagnetic (AFM) case, the spin-degeneracy remains sufficiently far away from the surface. Due to the increase of the magnetic structure period normal to surface, the AFM Brillouin zone (BZ) is reduced in this direction in comparison with the ferromagnetic (FM) (or PM) BZ, resulting in a backfolding of the bulk energy bands. These "umklapped" bands are narrowed by the exchange interaction, such that energy gaps open near the boundary of the AFM BZ. The size of these gaps is of the order of the magnetic exchange energy. If the latter is sufficiently large, the electronic structure of the AFM multilayer system can, therefore, be described as a manifold of narrow states of specific symmetry separated by wide energy gaps. As is well known (cf., e.g., Ref. 17), the existence of bulk energy band gaps, whether genuine or symmetry specific, can induce surface states, which are located spatially in the surface region and energetically in the band gap.

In spite of the variety and complexity of the electronic properties of magnetic MS, we first attempt to uncover general characteristic features of the surface electronic structure by means of rather simple tight-binding analytical calculations for a semi-infinite chain of magnetic atoms with FM or AFM coupling. This simple model with only a single orbital is useful, because it represents the projection of a real system onto the special case of surface-parallel wave vector $\mathbf{k}_{\parallel} = 0$ and of some selected state symmetry type, and because bulk states with a given $\mathbf{k}_{\parallel}$ and symmetry are—for a given effective one-electron potential—affected independently by the surface. It is noteworthy that the practical usefulness of a similar single-orbital-per-site approach was already demonstrated in an application to superlattice systems (cf. Ref. 18 for theoretically predicted Tamm-like surface states and Ref. 19 for their experimental observation). In this paper, the modulation of the potential is caused by the magnetic structure instead of the different materials in the superlattice.

To obtain more quantitative information on magnetic surface states and to explore their manifestation in photoemission, we have employed a relativistic multiple-scattering formalism to calculate the bulk and surface electronic structure, as well as spin-resolved and

dichroitic photoemission for a prototype system consisting of FM- or AFM-coupled ferromagnetic Fe monolayers and a varying number of Pt spacer layers. We chose Fe/Pt(001), rather than the more popular system Co/Cu(001), because the large magnetic moment of Fe and the large spin-orbit coupling of Pt in conjunction with the hybridization of Fe d states with Pt d states should lead to stronger effects, in particular, stronger magnetic dichroism. Furthermore, FePt is of interest because there are open questions concerning its magnetic structure. While self-consistent linear muffin-tin orbital (LMTO) calculations for the bulk (Ref. 20 and our present work) favor a ferromagnetic ground state (at $T = 0$), polar Kerr rotation angle spectra calculated for ferromagnetic ordering[21] were found to be substantially larger than their experimental counterparts measured at room temperature.[22] Since a bulk antiferromagnetic state is rather close in total energy, this suggests that some antiferromagnetic coupling might actually occur, either as a surface effect or in the form of a coexistence of ferromagnetic with thermally excited antiferromagnetic regions.

The paper is organized as follows. Section II is devoted to existence condition and main properties of magnetic surface states for a semi-infinite chain model in terms of a tight-binding Green function approach. In Sec. III, we briefly recall a relativistic layer-KKR formalism, specify the geometry and potential input for our calculations, and then present and discuss numerical results for the layer-, spin-, and symmetry-resolved densities of states and for spin-resolved normal photoemission spectra by circularly polarized light.

II. MODEL CALCULATIONS

In spite of the complicated interrelations between structural, magnetic, and potential characteristics in multilayer systems, we will be attempted to perform a reasonable picture of the electron structure, mostly affected by the perpendicular magnetic modulation, in terms of a one-dimensional chain with a single atomic orbital at each lattice site. The sensibility of such a simple one-dimensional approach is supported by the following arguments. First, it concerns the spatial distribution of the magnetic modulation of the system in question, where the local magnetic moments are aligned along the surface normal. Therefore, comparing electron scattering in the PM system (FM system) with that in the AFM system, one can conclude that the electrons with a certain spin projection in the AFM system suffer an additional scattering, due to the spin-dependent modulation of the effective potentials. It means, in particular, that the electrons are subject to the influence of the magnetic potential wells in the region close to the surface, which appear due to the truncation of the one-dimensional magnetic modulation at the surface.

In the AFM system the period of the magnetic scattering potentials is twice as large as in the FM system, which leads to the aforementioned effects of band narrowing on one hand and arising of AFM gaps on the other. Obviously, these additional scattering processes have essentially one-dimensional character, and only in this sense the label "one-dimensional" will be intentionally used, although the importance of the intralayer electron scattering, leading to the usual dispersion (i.e., $\mathbf{k}_{\|}$ dependence) of the surface electron structure, may not be diminished.

We assume equidistant spacing of the atoms, with a being the lattice constant. Furthermore, orbitals $\mid n,\tau\rangle$, which can be completely characterized by their lattice site, $n \in \mathcal{N}$, and their spin, $\tau = \pm$, on different sites are orthogonal. The on-site integrals ϵ

$$\epsilon \equiv \langle n,\tau \mid V^0 - V^{\text{atom}} \mid n,\tau\rangle, \tag{1}$$

are identical for all orbitals. Taking into account only next-neighbor interaction, the intersites hopping matrix elements read

$$\begin{aligned} t_{n\tau,n'\tau'} &\equiv \langle n,\tau \mid V^0 - V^{\text{atom}} \mid n',\tau'\rangle \\ &= \begin{cases} t & \mid n-n' \mid = 1 \\ 0 & \text{otherwise,} \end{cases} \end{aligned} \tag{2}$$

where V^0 (V^{atom}) is a one-particle Coulomb potential of the infinite chain (isolated atom). The magnetic exchange is incorporated into the Hamiltonian via a Zeeman term, $B\sigma_z$. In our model calculations, we ignore spin-orbit coupling.

The Hamiltonian of the bulk system (one-dimensional infinite closed chain) reads

$$\begin{aligned} H^{(0)} = &\sum_{n,\tau=\pm} \mid n\tau\rangle(\epsilon + B_n\tau)\langle n\tau \mid \\ &+t \sum_{n,\tau=\pm} (\mid n\tau\rangle\langle n+1,\tau \mid + \mid n+1,\tau\rangle\langle n\tau \mid). \end{aligned} \tag{3}$$

For the ferromagnetic system, the local magnetization is given by $B_n = B$, whereas for the antiferromagnetically ordered system, we have

$$B_n = \begin{cases} +B & \text{for even } n \\ -B & \text{for odd } n, \end{cases} \tag{4}$$

B being the exchange energy. Note, that the unit cell of the AFM system is twice as large as that of the FM system. The Hamiltonian possesses two important symmetries: it remains unchanged, if, first, the local exchange and the spins are reversed ($B \to -B$ and $\tau \to -\tau$), or if, second, the lattice index is increased by one and the spin is reversed ($n \to n+1$ and $\tau \to -\tau$).

Solving the Schrödinger equation with $H^{(0)}$ from Eq. (3), we obtain the bulk band structure for the FM system as

$$E_{k\tau} = \epsilon + \tau B + 2t\cos(ka), \tag{5}$$

i.e., the FM bulk band structure is that obtained in the paramagnetic case ($B = 0$), but exchange split by $2B$. The lower band is associated with "majority" states, the upper with "minority" states. The BZ is given by $k \in [0, 2\pi/a]$.

In the case of the AFM system, we arrive at

$$E_{k\lambda\tau} = \epsilon + \lambda\sqrt{B^2 + 2t^2[1+\cos(2ka)]}, \quad (6)$$

where $\lambda = \pm$ enumerates the AFM bands. Note that $E_{k\lambda\tau}$ is independent of the spin τ, due to the macroscopically vanishing magnetization. Because of the enlarged unit cell (with respect to that of the FM system), we are concerned with an umklapp process, i.e., the BZ is given by $k \in [0, \pi/a]$. Furthermore, in contrast to the paramagnetic system, which shows also macroscopically zero magnetization, there is band gap of width $2B$, which is due to the local exchange B.

Because the PM case is identical to FM case at $B = 0$, which has been studied in detail in the literature (cf. Ref. 27), we focus, in the following, exclusively on the AFM case. The complete information of a system can be obtained from it's Green function $G = (E - H)^{-1}$. A standard resolvent technique (see Refs. 17, 23–34 for the actual and related topics) leads to the surface Green function,

$$\langle 0,\tau \mid G(E) \mid 0,\tau\rangle = -\frac{2}{t}(X+\tau Y)\{\xi_1 - \xi_2 - \sqrt{\xi_1(\xi_1+\xi_2+2)} + 4\left[X_s + \tau(Y_s - Y)\right]\left[X+\tau Y\right]\}^{-1/2}, \quad (7)$$

where the reduced energy $X \equiv (E-\epsilon)/2t$, $Y \equiv B/2t$, $X_s \equiv (\epsilon_s - \epsilon)/2t$ is a measure of the difference between surface and bulk Coulomb integrals, $Y_s \equiv B_s/2t$ stands for the reduced surface Zeeman half splitting, and

$$\xi_{1,2} = Z \mp \mathrm{sgn}(Z)(Z^2-1)^{1/2}, \quad (8)$$

with $Z \equiv 2(X^2 - Y^2) - 1$. The roots of the denominator in Eq. (7) correspond to the positions of the surface states, provided that the energy E is out of the band range, i.e., $-Y < X < Y$ or $X < -\sqrt{Y^2+1}, X > \sqrt{Y^2+1}$. Within the antiferromagnetic gap, i.e., $-Y < X < Y$, the existence condition of the surface states reads

$$X_s < Y - Y_s \quad \text{or} \quad \epsilon_s + B_s < \epsilon + B. \quad (9)$$

There is a second surface state within the AFM gap corresponding to the opposite-spin projection. The splitting of these surface states is of the order of the bulk exchange splitting $2B$ at small surface relaxation, i.e., $\epsilon_s \approx \epsilon$ and $B_s \approx B$.

In the energy ranges $X < -\sqrt{Y^2+1}$ and $X > \sqrt{Y^2+1}$, i.e., the "outer" energy ranges, the corresponding surface state existence condition reads

$$X_s + Y_s > Y + \frac{1}{2\left(Y + \sqrt{Y^2+1}\right)},$$

or

$$\epsilon_s + B_s > \epsilon + B + \frac{2t}{2\left(B + \sqrt{B^2+4t^2}\right)}. \quad (10)$$

The energy splitting between these surface states is $2\sqrt{B^2+4t^2}$ for small relaxation.

The energetic splitting of the surface states appearing within the AFM gap is close (and indeed proportional) to the surface exchange, whereas the splitting of the surface states, which arise in the outer range, exceeds the surface exchange by a value of $2t^2/(B + \sqrt{B^2+4t^2})$.

Some specific properties of the surface electronic structure of the AFM system can be easily revealed from Eq. (7) for the surface layer (and in a similar manner for the other layers) and figured out in terms of the spin-resolved layer density of states (LDOS). In the following considerations, we have chosen $\epsilon = 0$ eV, $B = 1$ eV, and $t = 0.5$ eV, e.g., $Y = 1$. The imaginary part of the energy, η, is set to 0.01 eV.

In Fig. 1, we present the bulk band structure of the AFM system together with the LDOS of bulk (B) and surface located layers ($S, \ldots, S-3$). The surface Coulomb integral ϵ_s is set to ϵ. As is evident from our analytical considerations, the surface states are spin polarized and are strongly located at the first three surface layers, the largest contribution at the first layer (S). If the surface exchange splitting is reduced with respect to that of the bulk (for example, $B_s = 0.6B$), the surface states lie within the AFM gap, i.e., the reduced-energy range from -1 up to $+1$. For a small surface relaxation, i.e., $B_s = 1.2$ eV, we observe a surface resonance, which shows a rather large LDOS at the third layer. For an increased surface exchange energy ($B_s = 1.8$ eV), the surface states show up to lie in the outer range, i.e., $X < -\sqrt{2}$ or $X > \sqrt{2}$. Due to the symmetry of the Hamiltonian, the LDOS of bulk sites with an even layer index and spin τ is that for those of sites with an odd index and spin $-\tau$. The energy of the surface states as a function of the surface exchange splitting and surface Coulomb integral shows an almost linear dependence of their position on the surface exchange energy B_s. This holds for various values of ϵ_s and is in line with our analytical results.

Additional calculations for n ferromagnetically coupled layers, i.e., thin films, on an antiferromagnetically coupled substrate, show n states, which are confined to the thin film. The thin film states evidently occupy the energy range of the FM bulk bands.

III. RELATIVISTIC LAYER-KKR APPROACH

A. Model specifications

The present numerical calculations are based on a fully relativistic layer-KKR (LKKR) formalism for magnetic half-space crystalline systems allowing for overlayers and an arbitrary set of atoms with arbitrary magnetization in the unit cell of each two dimensionally periodic monolayer (cf. Ref. 35 and references therein). We briefly recall some of its key features. It relies on the muffin-tin approximation, which should be reasonable for close-packed metallic systems.

The muffin-tin potential input for the LKKR calculations was obtained from bulk potentials, which we calculated self-consistently, using the LMTO-ASA method. For Fe, this was done for a hypothetical fcc-Fe lattice, with the Pt lattice constant. The resulting spin magnetic moment per atom is $2.70\mu_B$ and $2.40\mu_B$ in the FM and

AFM phases, respectively. For Fe/Pt_n, $n = 1, 2$, we performed LMTO calculations for a large unit cell, which includes the FM or AFM coupled Fe layers, as well as the Pt spacer layers. The latter were allowed to become magnetically polarized by the adjacent Fe layers. Self-consistency was reached for prescribed FM or AFM coupling. The bulk magnetic moments in Fe/Pt system on Fe (Pt) thus obtained are $M_{Fe} = 2.80\mu_B$ ($M_{Pt} = 0.25\mu_B$) for the FM ordering and $M_{Fe} = 2.84\mu_B$ ($M_{Pt} = 0.13\mu_B$) for the AFM ordering. Similar values have been derived for the moments in the Fe/Pt_2 system on Fe (Pt) sites: $M_{Fe} = 2.80\mu_B$ ($M_{Pt1} = M_{Pt2} = 0.29\mu_B$) for the FM ordering and $M_{Fe} = 2.83\mu_B$ ($M_{Pt1} = -M_{Pt2} = 0.18\mu_B$) for the AFM ordering. Note that the amplitudes of the magnetic moments on Fe sites of Fe/Pt_n, $n = 1, 2$ systems are almost independent on the nearly nonmagnetic spacer (Pt) thickness and their magnetic interlayer ordering.

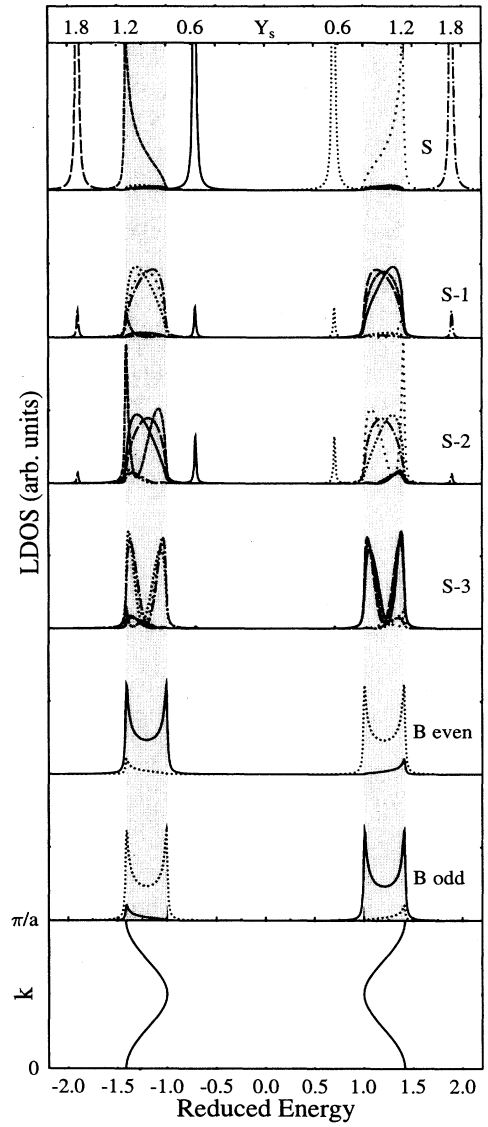

FIG. 1. Spin-resolved layer density of states of the one-dimensional AFM model system, for the first four surface layers ($S, \ldots, S-3$) and the bulk layers (B, even and odd layer index). Three values of the reduced surface exchange splitting, $Y_s = 0.6$ (solid for $\tau = +$ and fine dotted for $\tau = -$), $Y_s = 1.2$ (dashed for $\tau = +$ and broken dotted for $\tau = -$), $Y_s = 1.8$ (fine dashed for $\tau = +$ and dotted for $\tau = -$), τ being the spin projection. The surface exchange splitting is indicated at the surface state position (see top panel). In the first case, surface states are located within the AFM gap, whereas in the second these interfere with bulk states (surface resonances). In the last case, surface states are located outside of the band range. In the lowest panel the bulk band structure is shown. The energy scale refers to the reduced energy X.

Hole-lifetime effects are included in LKKR from the start via an imaginary part of the inner potential. The information on the occupied states (in the quasihole sense) is contained in a Green function matrix $G_{nN,n'N'}(\mathbf{k}_\parallel, E)$, where N and N' enumerate the monolayers, and n and n' refer to the basis atoms in the two-dimensional unit cell. The $\mathbf{k}_\parallel$-, layer-, and symmetry-resolved density of states (LDOS) is then

$$N_{nN,S}(\mathbf{k}_\parallel, E) = -\frac{1}{\pi} \lim_{\eta \to 0^+} \mathrm{tr}\, \mathrm{Im} \langle S \mid G_{nN,nN}(\mathbf{k}_\parallel, E + i\eta) \mid S \rangle, \quad (11)$$

where S gives the symmetry type, e.g., basis functions of the irreducible representations of the appropriate magnetic double group [e.g., for $\mathbf{k}_\parallel = 0$ and magnetization $\mathbf{M}$ normal to a (001) surface, the one associated with the magnetic single group $4\overline{m}m$]. Further projections onto spatial symmetry types and spin orientation relative to $\mathbf{M}$ are useful. We note that due to spin-orbit coupling dominantly majority-spin, LDOS features are generally accompanied by (smaller) minority-spin ones, and vice versa.[36]

The hole Green function G is used secondly for photoemission, within the one-step model, in relativistic dipole-transition matrix elements to a time-reversed LEED state $\langle \mathbf{r} \mid \Psi^\tau_{\mathbf{k}_\parallel, E} \rangle$, describing the photoelectron with spin τ at the detector by a 2×2 spin-density matrix

$$\rho_{\tau,\tau'} = \frac{1}{2i} \left(\tilde{\rho}_{\tau,\tau'} - \tilde{\rho}^\star_{\tau',\tau} \right), \quad (12)$$

where

$$\tilde{\rho}_{\tau,\tau'}(\mathbf{k}_\parallel, E) = -\frac{1}{\pi} k \int \mathrm{d}\mathbf{r} \int \mathrm{d}\mathbf{r}' \langle \Psi^\tau_{\mathbf{k}_\parallel} \mid \mathbf{r} \rangle \Delta \times G(\mathbf{r}, \mathbf{r}', \mathbf{k}_\parallel, E - \hbar\omega) \Delta^+ \langle \mathbf{r}' \mid \Psi^{\tau'}_{\mathbf{k}_\parallel} \rangle, \quad (13)$$

and the interaction of the electron with a monochromatic electromagnetic field $\mathbf{A}(\mathbf{r}) \exp(i\omega t)$ is expressed through the Dirac matrix $\hat{\alpha}$ as $\Delta = \hat{\alpha}\mathbf{A}$. We use the dipole approximation, i.e., $\mathbf{A}$ spatially constant. Magnetic dichroism is characterized by the change of the photoemission intensity upon reversal of the magnetization.

As a prototypical magnetic multilayer system, we choose Fe/Pt_n, where $n = 0, 1, 2$. Along the [001] direction, there are ferromagnetically magnetized Fe monolayers separated by n Pt monolayers. The bulk geometry is

simple tetragonal with an appropriate atomic basis. Concerning the exchange coupling between the Fe layers, we investigate both the ferromagnetic and the antiferromagnetic case. The semi-infinite system with (001) surface is taken as a truncated bulk with a Fe monolayer at the surface. The magnetization axis is chosen as [001], i.e., normal to the surface, which allows a fairly simple interpretation of the influence of spin-orbit coupling, since the magnetic electronic states can still be classified in terms of the irreducible representations of the (nonmagnetic) double group associated with the single group $4mm$, i.e., C_{4v} in Schönflies notation. Further, perpendicular magnetic anisotropy is likely to be more relevant for practical purposes. Variation of the number of monolayers constituting the Pt spacer layer reveals the influence of the magnetic period (i.e., the effects of multiple BZ backfolding) on the number and the energies of magnetic surface states and on magnetic circular dichroism (MCD) in photoemission.

To reach maximal information on the occupied electronic states — for $\mathbf{k}_{\|} = 0$ — we calculate simultaneously the bulk band structure along [001], spin-, symmetry-, and $\mathbf{k}_{\|}$-resolved layer densities of states (LDOS) and photoemission spectra. For the latter, we choose circularly polarized light at normal incidence, which gives rise to MCD. The real and imaginary parts of the uniform inner potential V_0 for the occupied states are taken as 12.2 eV and -0.02 eV in the LDOS calculations, respectively. In the photoemission calculations, however, we used linear increasing (in absolute value) imaginary parts. For the lower states, we chose $\mathrm{Im}V_0 = 0.025(E - E_F)$, for the upper states $\mathrm{Im}V_0 = -0.06(E - E_F)$, E_F denoting the Fermi energy.

For the surface potential barrier, we adopt the simplest model of a step function. As is known from earlier work (see Ref. 38), this model is, for a suitable choice of the step location, capable of correctly reproducing the positions of occupied surface states (below E_F). In the absence of a self-consistent determination of both surface barrier and surface magnetization together, we take the surface magnetic moment and the step position as parameters to be ultimately adjusted such as to reproduce surface state position determined by photoemission experiments. As our numerical LKKR calculations show, however, the surface state positions are far more sensitive to possible enhancements of the surface magnetic moments than to changes of the surface barrier position within physically reasonable limits. This can be made plausible by regarding the surface barrier roughly as a potential well of finite depth in front of the muffin-tin potential of the atomic layers. The width a of this well is determined by the position of the actual surface barrier, and its (spin-dependent) depth U is essentially governed by the amplitude of the magnetization in the topmost atomic layer. An elementary calculation for typical values $a < 0.5$ Bohr and U of about 0.2 Ry shows that the energy of electron states in this well is proportional to the depth U, with a entering only in a small correction term. This implies that surface states depend far more weakly on reasonable changes of the surface barrier location than on changes of the surface magnetization.

B. Layer density of states of Fe(001)

As the first and most basic system in our series $\mathrm{Fe/Pt}_n$, we take, for $n = 0$, a hypothetical fcc Fe with a lattice constant 3.88 Å terminated by a (001) surface. This system may be viewed as obtained by epitaxial growth of Fe on a Pt(001) substrate. Although perhaps less realistic than, e.g., the intensely studied system Fe/Cu(001) (see, for example, Ref. 37 and references therein), it exhibits qualitatively the same features and is more adequate for a systematic study of effects produced by the introduction of Pt spacer layers. We investigate the following three magnetic phases of this fcc Fe: (i) nonmagnetic (PM) phase and phases with (ii) ferromagnetic and (iii) antiferromagnetic interlayer coupling of ferromagnetically magnetized monolayers.

Figure 2 shows the band structure for these phases normal to the surface, i.e., in the direction $\Gamma - Z$ of the AFM BZ. Bands and electronic states are characterized by the four double-group symmetry types $\Delta_6\pm$ and $\Delta_7\pm$. For the sake of clarity and without any restriction of generality, our further analysis focuses on states with dominant spatial parts of Δ^5 single-group symmetry, which provide the main contributions in the important cases of normal photoemission by s polarized and by normally incident circularly polarized light. We denote the corresponding contributions to the LDOS for $\mathbf{k}_{\|} = 0$ by

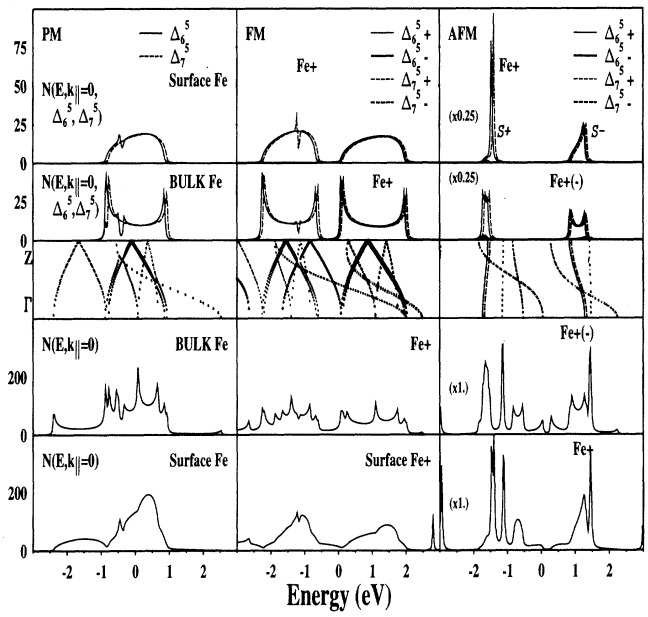

FIG. 2. Fe(001) (fcc with Pt lattice constant) in paramagnetic (left-hand column), ferromagnetic (central column), and antiferromagnetic (right-hand column) phase with perpendicular magnetization. *Central row of panels*: bulk band structure normal to the surface, with bands of Δ_6^5 and Δ_7^5 symmetry drawn in the case of AFM by solid and dashed lines, respectively; *lower two rows*: complete bulk and surface layer-DOS for $\mathbf{k}_{\|} = 0$; *upper two rows*: LDOS contributions of spin-up (down) $\Delta_6^5 + (-)$ and $\Delta_7^5 + (-)$ symmetry, with surface states marked as S±.

Δ_6^5 and Δ_7^5 (see top panel of Fig. 2). In the nonrelativistic (without spin-orbit coupling) limit they become double degenerate, with symmetry Δ^5. In the FM case, the PM electron states with Δ_6^5 and Δ_7^5 symmetry are seen to be simply spin split by the exchange interaction, as one would expect. For AFM interlayer coupling, the umklapped bulk bands become split at the BZ boundary and strongly narrowed, while retaining their spin degeneracy. As is demonstrated in Fig. 2, in the surface LDOS, the van Hove singularities have disappeared in all cases. For AFM, there are in addition very pronounced surface states, which are clearly split off the bulk LDOS and bands. The energy distance between lower Δ_6^5+ (Δ_7^5+) and upper Δ_6^5- (Δ_7^5-) states (about 2.8 eV) is directly related to the exchange splitting on the surface. Here, + and − stand for the global-frame spin projections normal to the surface, i.e., parallel and antiparallel to the magnetization of the surface layer. The angular parts of the basis orbitals of these symmetries, are of d_{xz} and d_{yz} types, i.e., they are essentially spatially distributed in planes normal to the surface (assumed as z axis) and are obviously sensitive to the magnetic structure along the surface normal. The influence of spin-orbit coupling, leading particularly to the separation of the nonrelativistic Δ^5 into Δ_6^5 and Δ_7^5 states, is rather weak (about 0.07 eV) in the case of Fe, as can be seen by the split van Hove singularities in Fig. 2.

The evolution of the bulk LDOS of symmetry Δ_6^5 to the surface LDOS is presented in more detail in Fig. 3. To demonstrate the usefulness of tight-binding calculations for a semi-infinite one-dimensional chain discussed in Sec. II, we also show results obtained (without spin-orbit coupling) by this simple method. The parameters of the latter were chosen to fit the LKKR bulk bands of symmetry Δ_7^5: hopping integral $t = 0.39$ eV, local magnetic half splitting $B = 1.17$ eV. For the LDOS, an inverse hole lifetime $\eta = 0.02$ eV [cf. Eq. (11)] was chosen in both cases. As can be seen in Fig. 3, for the individual layers (from bulk to surface), the LDOS results obtained by the two methods are almost identical. This indicates the essentially one-dimensional character of the spatial extension of the "interference states"[17] (which become surface states in the AFM case).

If there is an additional FM monolayer at the surface, i.e., a thin FM film (consisting of two monolayers) on the AFM substrate, there are two magnetic majority-spin surface states (see Fig. 4) instead of the one shown in Fig. 3. Let us first consider the case that the magnitude of the magnetization in the two top layers is equal to the bulk value M_0. As is seen in the left-hand column of Fig. 4, one majority surface state is below and the other above the lower-energy bulk band. Corresponding minority-spin surface states (not shown) occur around the higher-energy bulk band. Thus, a majority/minority pair of surface states resides within the AFM gap, and another pair is located exterior to the AFM band range.

The two top FM monolayers are now given enhanced magnetizations described by $M_1 = 2M_0$ (first layer) and $M_2 = 1.3M_0$ (second layer). As the right-hand part of Fig. 4 shows, the two majority-spin surface states are considerably shifted towards lower energies and they are

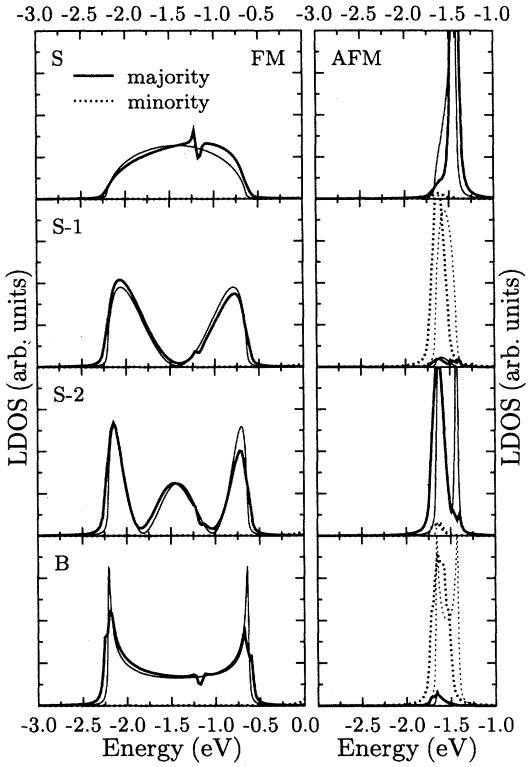

FIG. 3. Fe(001) with perpendicular magnetization FM (left-hand column) and AFM (right-hand column): occupied LDOS of Δ_7^5 symmetry for bulk and surface layers as obtained by relativistic layer-KKR (thick lines) and one-dimensional tight-binding (thin lines) calculations.

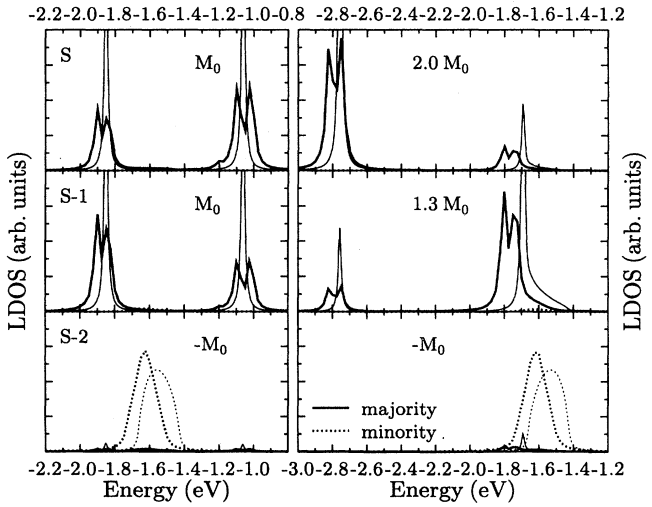

FIG. 4. Fe(001): same as AFM part of Fig. 3, but for a system with two FM-coupled monolayers at the surface followed by AFM-coupled monolayers. In the left-hand column of panels, the magnitude of the magnetization in each monolayer has the bulk value M_0. In the right-hand column, the magnetization of the first and the second monolayer is enhanced by 100% and by 30% relative to the bulk value M_0.

wider apart from each other. The minority-spin surface states (not shown) are correspondingly shifted towards higher energies. The distance between the majority and minority partners in each pair scales approximately linearly with the averaged surface magnetization (see Sec. II).

Noting the agreement between the linear chain results and the layer-KKR results, also for the above cases involving two FM top monolayers, we would like to emphasize that this was reached without fitting any further parameters, such as surface tight-binding parameters. Since the simple model calculations, using the one-dimensional version of the Green function method of Ref. 23, can be rapidly done on a personal computer, they are useful in exploring in detail the influence of variations of the magnetic structure on the surface electronic structure.

C. Layer density of states of $Fe/Pt_n(001)$

The introduction of Pt spacer layers involves three types of effects. First, the unit cell normal to the surface is increased by a factor $n + 1$, which entails increased backfolding (umklapp) of bands and consequently more gaps and separated AFM bands. Second, the chemically different species Pt complicates the band structure. Third, the large atomic number of Pt together with a strong hybridization of the Fe states with the Pt states leads to much stronger spin-orbit coupling effects.

For $Fe/Pt_1(001)$, bulk bands and LDOS below E_F are shown in Fig. 5. The electron states of the FM phase on the surface are fairly smoothed in comparison with their bulk counterparts. For the AFM phase, there are now two mainly Fe bands with dominant Δ_6^5 and Δ_7^5 symmetry (instead of one for pure Fe) and consequently two majority-spin surface states (labeled S_1+ and S_2+). Also, in contrast to the pure Fe case, the spin-orbit splitting between Δ_6^5 and Δ_7^5 symmetry types is now fairly large (about 0.4 eV). These features might be observable in angle-resolved photoemission measurements, where each symmetry type of the electron states can be explored by using an appropriate light polarization and geometrical setup. In particular, the use of right (left) circularly polarized light makes possible the resolution between magnetically split $\Delta_6^5\pm$ ($\Delta_7^5\pm$) states.

As the thickness of the nonmagnetic spacer is increased, the corresponding enhancement of the local magnetic moment of Fe makes the amplitudes of the magnetic surface states more pronounced. This can be seen in Fig. 6 (only spin-majority counterpart is shown). The reduction of the Fe/Pt_2 AFM BZ, which is only 1/3 of that for Fe, gives rise to additional magnetic surfaces states. In the majority-spin range, there are two prominent ones, labeled S_1+ and S_2+. If the number of Pt layers increases further, there remain eventually only one majority- and one minority-spin surface state, i.e., the surface electronic structures approaches that of an isolated FM monolayer on a Pt substrate.

D. Photoemission

The above electronic structure and, in particular, the surface states of our sequence of $FePt_n$ systems mani-

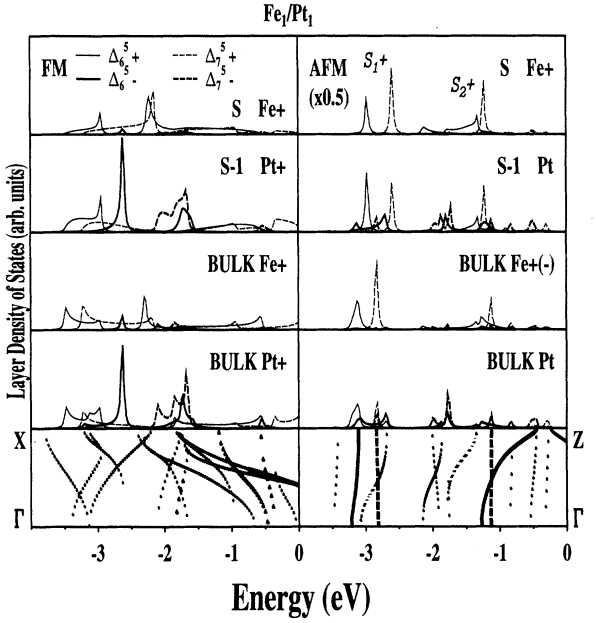

FIG. 5. Fe/Pt: *bulk band structure* $E(k_\perp)$ of FM and AFM phases (bottom panels); *symmetry- and* $(\mathbf{k}_\parallel = 0)$*-resolved LDOS*, Fe+ (Fe−) belong to the layer magnetized in (out of) the surface. For other notations see caption for Fig. 2.

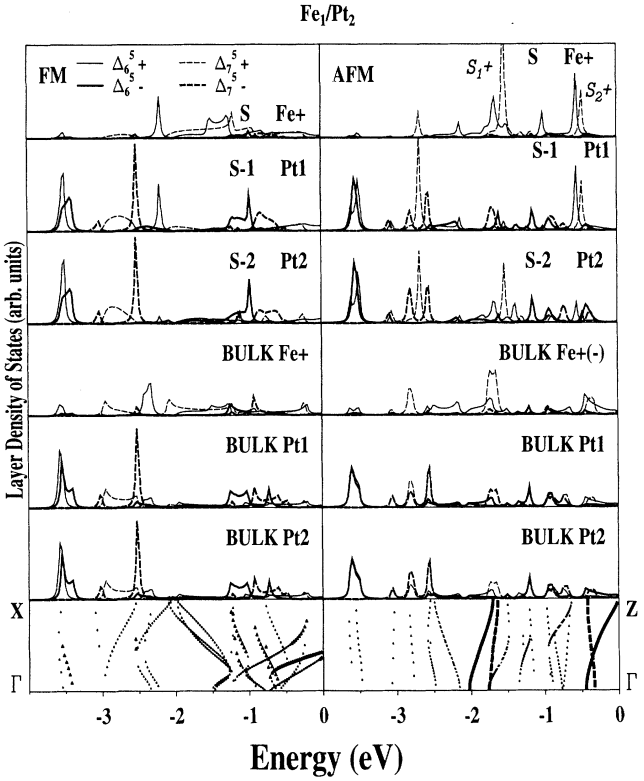

FIG. 6. Fe/Pt_2: analogous to Fig. 5.

fest themselves in greatest detail in spin-resolved (normal) photoemission by normally incident circularly polarized light. For normal incident right-handed circular polarized light and normal emission from a (001) surface, dipole selection rules imply in the nonmagnetic (or paramagnetic) case, that photoelectrons excited from initial states with Δ_6 symmetry (Δ_7 symmetry) show a complete spin polarization parallel (antiparallel) to the surface normal, i.e., $P_z = +1$ ($P_z = -1$). Reversal of the helicity changes P_z into $-P_z$, the intensity, however, remains unchanged, due to Kramer's degeneracy. In other words, right-handed circular polarized light detects only one part of the Kramer's doublet. Reversing the helicity detects the other (degenerate) part. In the magnetic case, Kramer's degeneracy is lifted and the initial states are themselves spin polarized, i.e., majority (minority) states with spin parallel (antiparallel) to the surface normal. Therefore, with right-handed circular polarized light one detects only the majority (minority) part of initial states with Δ_6 symmetry (Δ_7 symmetry). Thus, we expect that spin-polarized surface states can be observed only by one helicity of the incident light.

For fixed magnetization direction normal to the surface, there are four inequivalent partial intensity spectra I_τ^σ, where $\tau = \pm$ is the sign of the photoelectron spin-polarization direction and $\sigma = \pm$ refers to positive/negative helicity of the light. According to relativistic dipole selection rules, I_τ^+ is associated with initial states of symmetry Δ_6 and I_τ^- with Δ_7.

Spectra calculated for 21.2 eV photon energy are shown in Fig. 7. The simplest case is FM Fe (left-most column of panels): the relevant initial states have majority spin, and Δ_6 states are separated slightly from Δ_7 ones, due to a small spin-orbit interaction (as was shown in Fig. 2). Consequently, there are only I_+^+ and I_+^- spectra, which differ from each other, i.e., there is magnetic circular dichroism. (For details and references to earlier work on MCD, see Ref. 36.) In the AFM Fe case, there are two prominent spin-up peaks (labeled S^7 and S^6), which are associated with the surface state $S+$ in Fig. 2. In addition there are two spin-down peaks, due to oppositely magnetized deeper layers. The resulting MCD is seen to be much larger than in the FM Fe case.

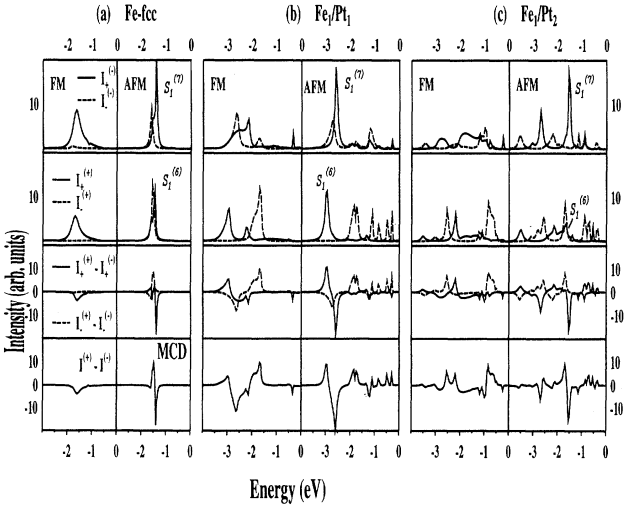

FIG. 7. *Spin-resolved normal photoemission intensity spectra* $I_\pm^{(\pm)}$ for (from left to right) Fe, Fe/Pt, and Fe/Pt_2 MS in their FM and AFM phases, photon energy $\hbar\omega = 21.2$ eV, subscripts of $I_\pm^{(\pm)}$ mean the spin projection, superscripts stand for right (left) circularly polarized light; lowest panel demonstrates MCD as the difference between spin-averaged $I^{(+)}$ and $I^{(-)}$ intensities.

For $FePt_1$ in the AFM phase, a large MCD originates from the majority surface states S_1. The distance between the opposite-sign peaks in the difference spectrum corresponds to the spin-orbit splitting, which is large due to the large atomic number of Pt ($Z = 78$).

For all three systems, MCD effects in the AFM-ordered phase exceed (with other conditions being the same) those in the FM phase. They are enhanced by and indeed owe their very existence to the magnetic surface states of symmetry types Δ_6 and Δ_7. The size of these surface states changes only weakly as the period of the magnetic structure normal to the surface is increased by increasing the number of nonmagnetic spacer layers. Since for a few spacer layers there remains only one dominant majority-spin surface state (of each symmetry type), and since elastic and inelastic scattering lead to a small escape depth of the photoelectrons, the limit case of a mono-atomic ferromagnetic overlayer on a nonmagnetic substrate is practically reached as the magnetic period becomes more than a few interlayer distances.

IV. CONCLUDING REMARKS

We have investigated the electronic structure of antiferromagnetically coupled layered systems first in terms of a tight-binding Green function approach for a simple model, and second by relativistic layer-KKR calculations for a more realistic effective one-electron potential. As the simple model system, we chose a one-dimensional semi-infinite chain with one atomic orbital per lattice site. An analytical Green function calculation resulted in explicit formulas for the existence of surface states and for their energy as a function of the tight-binding parameters, especially the surface Coulomb integral and the surface exchange energy. For the antiferromagnetically coupled system, spin-polarized surface states were found, the energy of which lies within (outside) the AFM bulk energy gap, if the surface exchange is reduced (enhanced) with respect to that of the bulk. The energy position of the surface states depends almost linearly on the surface exchange energy. Switching the AFM coupling between the outermost atoms to FM and leaving the remainder unchanged, Green function renormalization technique calculations revealed an extra surface state outside the gap, which does not exist in the original AFM coupled system. More generally, the number of surface states is proportional to the number n of FM-coupled monolayers in the surface region (with $n = 1$ corresponding to the simple AFM system).

Our expectations from general arguments and from our simple model calculations are corroborated by relativistic

layer-KKR calculations and carried out for $FePt_n(001)$ systems. In particular, n magnetic surface states occur for AFM systems, with n FM-coupled monolayers on top. Their energies are very sensitive to the size of the magnetization in these monolayers and more mildly so to physically reasonable variations of the surface barrier position. Since we have not determined surface magnetizations and surface barriers self-consistently, but regarded them as parameters to be adjusted by comparison with photoemission experiments, the present surface state energies are prototypical rather than real *a priori* predictions.

Due to spin-orbit coupling, the majority- and minority-spin surface states occur in pairs of double-group symmetry types Δ_6 and Δ_7, which are separated in energy. This separation is strongly enhanced by the presence of Pt layers, as a consequence of the large atomic number of Pt and the hybridization between Fe and Pt orbitals.

The manifestation of the surface states in photoemission was explored by relativistic calculations within the one-step model of photoemission. In general, the photoelectron intensity spectra exhibit spin-polarized peaks at the surface state energies. For circularly polarized light, the photoemission spectra, even if not spin resolved, depend on the helicity of the light, i.e., there is surface-induced MCD. Somewhat surprisingly, this MCD can even be stronger for AFM-coupled systems than for FM-coupled ones. Photoemission experiments employing spin analysis and/or circularly polarized light, are therefore recommended for the study of AFM-coupled multilayer systems with perpendicular magnetization. Specifically for the magnetic structure problem of FePt addressed in the Introduction, an experimental search for our surface states and their magnetic dichroism might reveal the presence of AFM-coupled regions. In making contact between our results and experimental data, in addition to having to adjust our parameters surface magnetization and surface barrier location, two restrictions have to be borne in mind. First, the measurement temperature has to be well below magnetic phase-transition temperatures. Second, the surface has to be rather perfectly ordered, since peculiar geometrical reconstructions like the one recently determined for ultrathin Fe films on Cu[37] can be expected to strongly affect the electronic structure.

ACKNOWLEDGMENTS

This work was supported by the Deutsche Forschungsgemeinschaft under Contract No. Fe198/2-1.

[1] *Magnetic Multilayers*, edited by L. H. Bennett and R. E. Wabon (World Scientific, Singapore, 1993).
[2] L. Baumgarten, C. M. Schneider, H. Petersen, F. Schäfers, and J. Kirschner, Phys. Rev. Lett. **65**, 492 (1990).
[3] J. E. Ortega, F. J. Himpsel, G. J. Mankey, and R. F. Willis, Phys. Rev. Lett. **47**, 1540 (1993).
[4] C. Carbone, E. Vescovo, O. Rader, W. Gudat, and W. Eberhardt, Phys. Rev. Lett. **71**, 2805 (1993).
[5] F. U. Hillebrecht, Ch. Roth, R. Jungblut, E. Kisker, and A. Bringer, Europhys. Lett. **19**, 711 (1992).
[6] K. Garrison, Y. Chang, and P. D. Johnson, Phys. Rev. Lett. **71**, 2801 (1993).
[7] D. Li, M. Freitag, J. Pearson, Z. Q. Qiu, and S. D. Bader, Phys. Rev. Lett. **72**, 3112 (1994).
[8] T. Kraft, P. M. Marcus, and M. Scheffler, Phys. Rev. B **49**, 11 511 (1994).
[9] J. Thomassen, F. May, B. Feldmann, M. Wuttig, and H. Ibach, Phys. Rev. Lett. **69**, 3831 (1992).
[10] B. T. Thole and G. van der Laan, Phys. Rev. B **48**, 9613 (1994).
[11] G. Y. Guo, H. Ebert, W. M. Temmerman, and P. J. Durham, Phys. Rev. B **50**, 3861 (1994).
[12] P. Bruno and C. Chappert, Phys. Rev. Lett. **67**, 1602 (1991); P. Bruno, Europhys. Lett. **23**, 615 (1993).
[13] P. Lang, L. Nordström, R. Zeller, and P. H. Dederichs, Phys. Rev. Lett. **71**, 1927 (1993).
[14] V. I. Safarov, V. A. Kosobukin, C. Hermann, G. Lampel, J. Peretti, and C. Marlière, Phys. Rev. Lett. **73**, 3584 (1995).
[15] K. M. Schep, P. J. Kelly, and G. E. W. Bauer, Phys. Rev. Lett. **74**, 586 (1995).
[16] R. Loloee, P. A. Schroeder, W. P. Pratt, J. Bass, and A. Fert, Physica B **204**, 274 (1995).
[17] S. G. Davison and M. Stęślicka, *Basic Theory of Surface States* (Clarendon Press, Oxford, 1992).
[18] M. Stęślicka, R. Kucharczyk, and M. L.Glasser, Phys. Rev. B **42**, 1458 (1990).
[19] H. Ohno, E. E. Mendez, J. A. Brum, J. M. Hong, F. Agullo-Rueda, L. L. Chang, and L. Esaki, Phys. Rev. Lett. **64**, 2555 (1990).
[20] M. Podgorny, Phys. Rev. B **43**, 11 300 (1991).
[21] S. V. Halilov and R. Feder, Solid State Commun. **88**, 749 (1993).
[22] T. Katayama, T. Sugimoto, Y. Suzuki, M. Hashimoto, P. de Haan, and J. C. Lodder, J. Magn. Magn. Mater. **104**, 1002 (1992).
[23] J. Henk and W. Schattke, Comput. Phys. Commun. **77**, 69 (1993); A. Bödicker, W. Schattke, J. Henk, and R. Feder, J. Phys. Condensed Matter **6**, 1927 (1994).
[24] J. Koutecký, Phys. Rev. **108**, 13 (1957).
[25] S. G. Davison and J. D. Levine, in *Solid State Physics: Advances in Research and Applications*, edited by H. Ehrenreich, F. Seitz, and D. Turnbull (Academic Press, New York, 1970).
[26] D. Kalkstein and P. Soven, Surf. Sci. **26**, 85 (1971).
[27] H. J. W. M. Hoekstra, Surf. Sci. **205**, 523 (1988).
[28] J. Kudrnovsky, I. Turek, V. Drchal, P. Weinberger, S. K. Bose, and A. Pasturel, Phys. Rev. B **47**, 16 525 (1993).
[29] D. A. Mirabella, C. M. Aldao, and R. R. Deza, Phys. Rev. B **50**, 12 152 (1994).
[30] S. Crampin, J. Phys. Condensed Matter **5**, 4647 (1993).
[31] G. Grosso, S. Moroni, and G. Pastori Paravicini, Phys. Scr. **T25**, 316 (1989).
[32] G. Wachutka, A. Fleszar, F. Máca, and M. Scheffler, J. Phys. C **4**, 2831 (1992).
[33] J. E. Inglesfield and G. A. Benesh, Phys. Rev. B **37**, 6682 (1988).

[34] H. L. Skriver and N. M. Rosengaard, J. Phys. Condensed Matter **4**, 2831 (1992).
[35] S. V. Halilov, E. Tamura, H. Gollisch, D. Meinert, and R. Feder, J. Phys. Condensed Matter **5**, 3859 (1993).
[36] T. Scheunemann, S. V. Halilov, J. Henk, and R. Feder, Solid State Commun. **91**, 487 (1994).
[37] S. Müller, P. Bayer, C. Reischl, K. Heinz, B. Feldmann, H. Zillgen, and M. Wuttig, Phys. Rev. Lett. **74**, 765 (1994).
[38] S. V. Halilov, H. Gollisch, E. Tamura, and R. Feder, J. Phys. Condensed Matter **5**, 4711 (1993); M. Lau, S. Löbus, R. Courths, S. Halilov, H. Gollisch, and R. Feder, Ann. Phys. (Leipzig) **2**, 450 (1993); S. Löbus, M. Lau, R. Courths, and S. Halilov, Surf. Sci. **287/288**, 568 (1993); S. Löbus, R. Courths, S. Halilov, H. Gollisch, and R. Feder, Surf. Rev. Lett. (to be published).

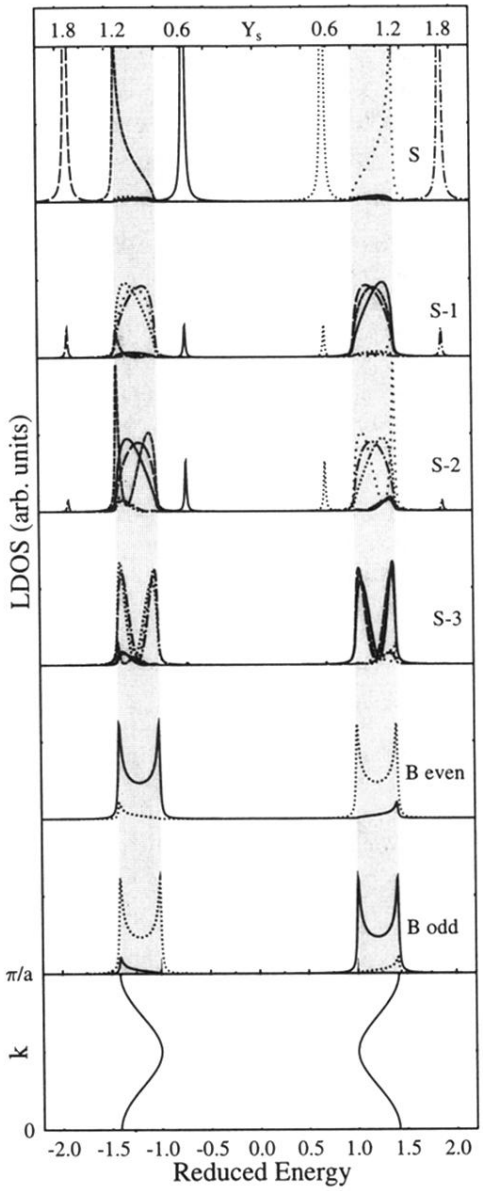

FIG. 1. Spin-resolved layer density of states of the one-dimensional AFM model system, for the first four surface layers ($S, \ldots, S-3$) and the bulk layers (B, even and odd layer index). Three values of the reduced surface exchange splitting, $Y_s = 0.6$ (solid for $\tau = +$ and fine dotted for $\tau = -$), $Y_s = 1.2$ (dashed for $\tau = +$ and broken dotted for $\tau = -$), $Y_s = 1.8$ (fine dashed for $\tau = +$ and dotted for $\tau = -$), τ being the spin projection. The surface exchange splitting is indicated at the surface state position (see top panel). In the first case, surface states are located within the AFM gap, whereas in the second these interfere with bulk states (surface resonances). In the last case, surface states are located outside of the band range. In the lowest panel the bulk band structure is shown. The energy scale refers to the reduced energy X.